buildings

MDPI

Article

How Time-of-Use Tariffs and Storage Costs Shape Optimal Hybrid Storage Portfolio in Buildings

Hong Tang [1,*], Yingbo Zhang [1] and Zhuang Zheng [2]

[1] Department of Building Environment and Energy Engineering, The Hong Kong Polytechnic University, Hong Kong 999077, China
[2] State Key Laboratory of Internet of Things for Smart City, Department of Electrical and Computer Engineering, University of Macau, Macau 999078, China
* Correspondence: honghong.tang@polyu.edu.hk

Abstract

Time-of-Use (TOU) tariffs are a primary driver for deploying demand-side energy storage, yet their specific structural characteristics, such as peak-to-valley ratios, and the presence of critical-peak pricing, can significantly influence the economic viability of hybrid storage systems. In addition, the continuous decrease in storage capacity costs also constitutes a major influencing factor on storage investment portfolios. This study investigates the sensitivity of optimal hybrid storage portfolios to varying TOU tariffs and storage costs. We develop a multi-scenario optimization framework that models diverse, realistic TOU tariff structures and evaluates their impact on the life cycle economic performance of hybrid storage in a representative office building. The methodology leverages a refined daily operation optimization model that accounts for storage degradation and system efficiencies, applied across a set of typical operational days. The impacts of specific tariff parameters (e.g., peak-to-valley ratio, critical-peak pricing) and storage costs on the optimal allocation of investment between battery and cooling storage are investigated. The thresholds of tariff and capacity cost that trigger a shift in investment preference are identified. The findings provide actionable insights for policymakers on designing effective dynamic tariffs to incentivize specific storage technologies and for building owners formulating future-resilient storage investment strategies.

Keywords: hybrid energy storage system; Time-of-Use tariff; optimal investment portfolio; life-cycle analysis; storage degradation

Check for updates

Academic Editor: Emilio Ghiani

Received: 1 December 2025
Revised: 16 December 2025
Accepted: 17 December 2025
Published: 22 December 2025

Copyright: © 2025 by the authors. Licensee MDPI, Basel, Switzerland. This article is an open access article distributed under the terms and conditions of the Creative Commons Attribution (CC BY) license.

1. Introduction

1.1. Research Background

In the global transition towards carbon neutrality and sustainable development, distributed renewable energy sources, particularly onsite solar photovoltaics (PV), are being integrated into modern power grids at an unprecedented rate. However, the inherent intermittency and uncertainty of these resources pose significant challenges to the stability and reliability of the power system [1]. The resulting "net load", the difference between total electricity demand and renewable generation, can exhibit steep ramps and high peaks, straining grid infrastructure and requiring costly fast-ramping reserves to maintain balance [2]. A critical solution to alleviate this stress and enhance system economy lies in leveraging demand-side energy flexibility through the local consumption and load-shifting capabilities of distributed energy resources [3]. As a core incentive for demand-side response, dynamic pricing mechanisms, particularly Time-of-Use (TOU) tariffs, have been

widely adopted. By setting higher electricity prices during peak demand hours and lower prices off-peak, TOU tariffs create a powerful economic motive for end-users to deploy energy storage systems for peak shaving and valley-filling arbitrage. Given that building operations account for a massive 28% of global final energy consumption in 2023 according to the International Energy Agency [4], the building sector possesses immense flexibility potential. Buildings are rapidly evolving from passive consumers into active prosumers by integrating distributed energy resources like rooftop PV and energy storage systems [5].

Deploying distributed energy storage offers a crucial dual benefit. For grid operators, it can absorb surplus renewable generation and discharge during periods of high demand, effectively smoothing the net load profile and reducing stability burdens. For building operators, this load shifting capability can be leveraged to significantly reduce energy costs under TOU tariffs. The economic situation is especially strong when cooling loads are increasing greatly. Hot summers result in substantial cooling energy demand, primarily for air-conditioning, which accounts for a large proportion of total building energy consumption and concentrates heavily during expensive daytime peak hours. This direct correlation with high electricity prices imposes a significant financial burden on building operation. Therefore, utilizing thermal storage systems to shift this massive cooling load from peak to off-peak periods offers substantial economic benefits [6]. Meanwhile, attention is also growing on electrical storage capable of directly shifting electrical loads. This application in building energy systems is accelerating, driven by the continuous decrease in storage capacity costs and the rising interest in the secondary use of retired electric vehicle batteries, i.e., second-life batteries [7]. Given the complex and diverse energy demands of modern buildings, the integration of hybrid energy storage systems (HESS) that combine battery energy storage systems (BESS) and thermal energy storage (TES) provides an integrated solution. This approach utilizes complementary strengths where batteries offer fast response for electrical fluctuations and price arbitrage, while TES efficiently manages the large cooling load with generally lower cost and longer life. However, determining the optimal investment allocation between these technologies is not straightforward. The optimal storage portfolio depends not only on the load and PV pattern, but also critically on the structure of the TOU tariff itself. Therefore, advanced design optimization is essential to maximize both the technical performance and economic returns of HESS under dynamic conditions.

1.2. Literature Review

Existing research has extensively investigated the optimal design of building integrated energy storage to enhance renewable self-consumption and economic performance. This review part first examines studies on individual storage technologies, then progresses to hybrid systems, ultimately highlighting the critical influence of TOU tariffs on their optimal configuration and identifying key research gaps. In the domain of BESS, numerous studies have focused on optimizing battery capacity in response to electricity prices. The work of Li et al. [8], for instance, revealed that the optimal sizing ratio for residential PV-battery systems is highly sensitive to the peak-to-valley price difference in TOU tariffs. Similarly, Zhang et al. [9] analyzed the economic performance of various PV-battery combinations under dynamic tariffs. Liu and Gou [10] established a structured technical pathway that encompasses hybrid forecasting model development, stability-oriented optimization design, and scenario-based performance evaluation. This framework provides an integrated solution for enhancing grid resilience and energy autonomy in residential PV-battery systems. However, a common limitation across existing studies is the inadequate consideration of battery degradation, which may lead to an overestimation of long-term returns from TOU arbitrage. Several studies [11,12] have attempted to integrate degradation

into optimization models to ensure realistic economic assessments, which shows that the mathematical programming model for battery optimization is challenging to solve, and the computational burden is heavy when considering the effect of battery degradation.

On the other hand, the implementation of active TES systems, such as chilled water tanks, ice storage, and phase change material storage, has been increasing globally. Chilled water storage coupled with heating, ventilation, and air-conditioning (HVAC) systems is considered as a promising storage solution due to low capital costs and fewer safety concerns [13]. Tarragona et al. [14] analyzed the economic and energy impacts of different compositions of PV–Heat pump–TES tank systems for various buildings in European cities of various climates. Zang et al. [15] developed a bilevel optimization method to solve the complex challenge of simultaneously sizing the water tank and determining its cooling supply strategy. Chen et al. [16] optimized both capacities of BESS and TES for buildings under different climate zones assuming a constant coefficient of performance (COP), which represents a simplification that may compromise the accuracy and real-world applicability of the optimization results. The non-linear characteristics of the coupled equipment (e.g., variable chiller efficiency with load and temperature) and the dynamic, uncertain nature of cooling demand would significantly increase the complexity of both the design and operational optimization problems [17]. The economic viability of demand-side storage is further governed by external market conditions, notably the structure of electricity tariffs, as well as storage capacity prices. Previous studies have not adequately addressed the challenges posed by the non-linearity of hybrid storage operation on the overall design optimization process, nor have they investigated the influence of TOU tariff variations and battery capacity prices on the resulting optimal design.

The complexity of designing and operating hybrid energy storage systems is significantly amplified by the highly variable and uncertain nature of both building energy loads and dynamic scenarios. Dealing with the life cycle of granular, high-resolution data (e.g., 8760 h of load and price data per year) directly in an optimization model can lead to an intractable computational burden [18]. To address this challenge, typical day analysis has emerged as a powerful and widely adopted data-driven dimensionality reduction technique in energy system research. Hemmati et al. [19] consider a working day and a weekend day in each season as representative days in the optimal operation problems for energy hub design. While it is effective for system design, how to choose the typical day for energy storage design remains uninvestigated. Therefore, numerous clustering algorithms are adopted to group a large set of daily or seasonal profiles (e.g., daily electricity demand, PV generation, or net load profiles) into a manageable number of representative scenarios or typical days in energy system design. Schütz et al. [20] compare different clustering methods (such as k-centers, k-means, k-medians, and k-medoids) for the selection of typical demand days and indicate these methods are able to determine energy systems that are close to the optimal system. This process effectively captures the essential variability and statistical characteristics of the original dataset while significantly reducing the number of timesteps that can be explicitly included in the optimization model.

Therefore, this study aims to fill the above-mentioned gaps by developing an optimization model that incorporates key performance degradation and dynamic efficiencies for energy storage systems and systematically investigating how different TOU tariffs and capacity costs shape the optimal hybrid storage investment portfolio in buildings. The findings are intended to provide more precise and reliable decision support for energy storage planning and policymaking. The main contributions of this paper include:

I Developing a life-cycle design framework for a hybrid storage system systematically considering the non-linear characteristics in operation.

I Investigating the impact of diverse TOU tariff scenarios on the optimal portfolio of hybrid storage for commercial buildings.

I Assessing the long-term economic robustness of different storage configurations under different storage capacity costs, providing forward-looking insights for making future-resilient investment decisions.

2. Methodology

2.1. Overall Framework

Figure 1 illustrates the framework of the life-cycle optimization method for hybrid storage systems. This methodology systematically integrates four key components: external data input, case building modeling, system configuration, and life-cycle operation optimization. The data input module incorporates the necessary information for modeling, specifically climate data (outdoor temperature and global horizontal irradiance) and the TOU tariff structure which acts as the primary external economic signals investigated in this study. The system configuration block defines the hybrid storage system, comprising both electrical storage and cooling storage components. This system interacts with the HVAC system and electrical/cooling loads. The life-cycle operation optimization process involves two stages: first, dynamic scheduling is performed via operation optimization of typical days to establish the year 1 model scheme. This operational scheme is then subjected to a long-term degradation model to simulate the system lifetime performance which accounts for component aging and replacement. This integrated life-cycle approach allows for the assessment using two key indicators including the life-cycle cost savings (LCCS) and the discounted payback period (DPBP), enabling a systematic determination of how the TOU tariff structure shapes the economically optimal hybrid storage portfolio.

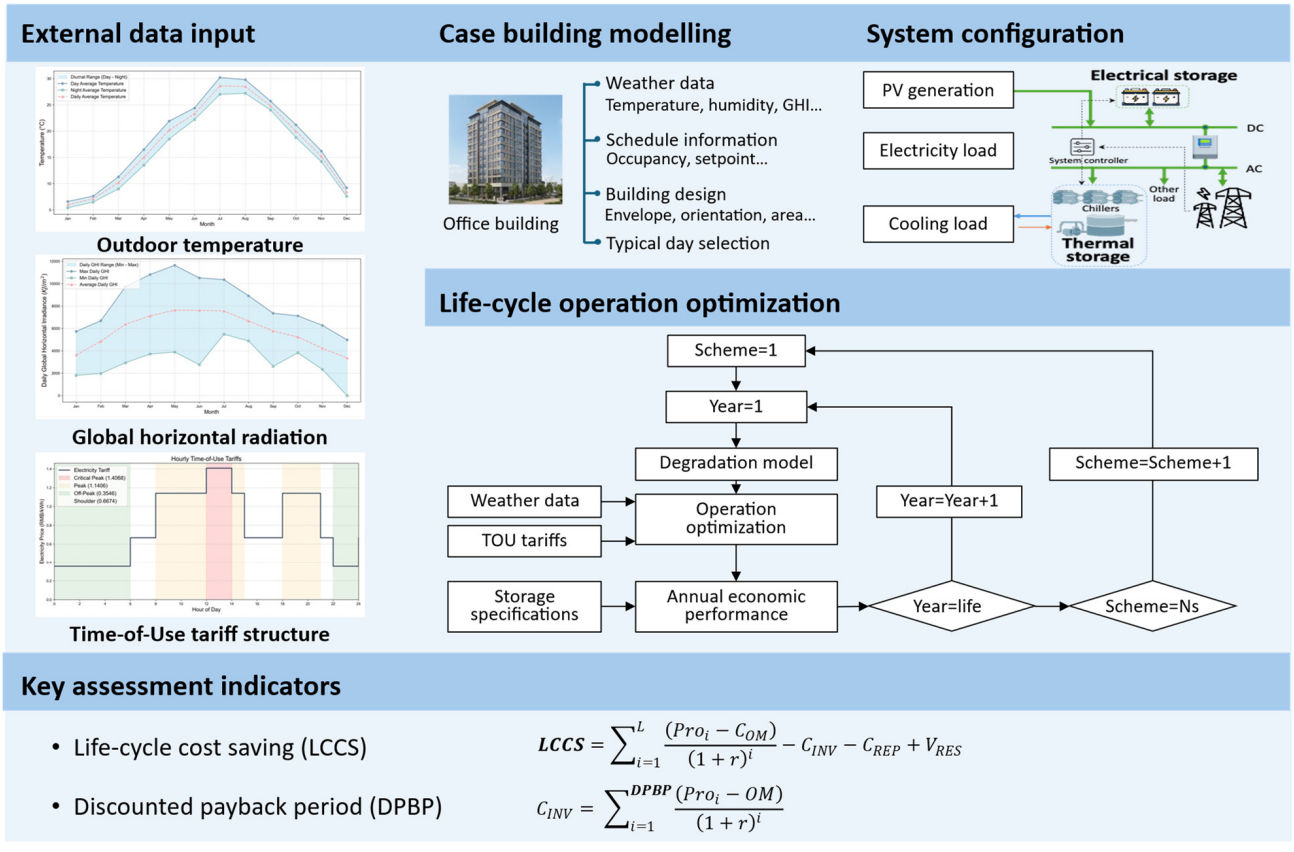


Figure 1. Framework of the proposed optimal design method for hybrid storage systems.

2.2. Daily Operation Optimization

The operational model aims to determine the most economical dispatch strategy for the hybrid storage system. This optimization is performed over a 24 h rolling horizon with a one-hour timestep. The final state of charge from one day serves as the initial state for the next, ensuring operational continuity. The core objective is to minimize the net daily electricity cost, as defined in Equation (1). This function calculates the total cost of power imported from the grid (at the TOU price, π_t^{TOU}) minus the total revenue from exporting surplus PV generation (at the Feed-in price, π_t^{FIT}). At each time t, the system must satisfy the primary energy balance in Equation (2), ensuring that grid power, BESS power, and PV generation match the HVAC and other building loads.

The BESS model is constrained by Equations (3)–(5). The state of charge is updated at each step based on the previous state, charge/discharge power, and round-trip efficiencies, as shown in Equation (4). The battery operation is bounded by its maximum rated power and its allowable state of charge (constrained for slowing the battery degradation).

Total HVAC power is the sum of the chiller, pump, and fan power as shown in Equation (6), where pump power is a function of cooling load and fan power is assumed constant. The cooling load is met by chillers and the cooling storage tank as shown in Equation (7). As shown in Equation (8), chiller power consumption is modeled as a piecewise quadratic function of its part-load ratio (PLR), with coefficients derived from regression analysis. It captures the chiller's non-linear efficiency curve while significantly enhancing the optimization solvability and computational speed. The PLR is an optimized variable, constrained by practical safe operational range. The meaning of each subject can be found in Abbreviations.

$$Cost = min \sum_{t=1}^{T} (\pi_t^{TOU} P_{grid,t} - \pi_t^{FIT} G_{grid,t}) \quad (1)$$

$$P_{grid,t} - G_{grid,t} = P_{HVAC,t} - P_{EES,t} - P_{PV,t} + P_{other,t} \quad (2)$$

$$P_{EES,t} = P_{EES,t}^{\wedge} - P_{EES,t}^{\vee} \quad (3)$$

$$SOC_{EES,t+1} = SOC_{EES,t} + \frac{\eta_{ch} P_{EES,t}^{\wedge} - P_{EES,t}^{\vee} / \eta_{dis}}{E_{EES}} \quad (4)$$

$$SOC_{min} \leq SOC_{EES,t} \leq SOC_{max} \quad (5)$$

$$P_{HVAC,t} = P_{ch,t} + P_{pump,t} + P_{fan,t} \quad (6)$$

$$q_{cooling,t} = PLR_t * q_{rated} - q_{TES,t} \quad (7)$$

$$P_{ch,t} = 0, \text{ or } P_{ch,t} = \left(n_1 {PLR_t}^2 + n_2 PLR_t + n_3 \right) * P_{ch,rated} \quad (8)$$

$$PLR_t = 0, \text{ or } PLR_{min} \leq PLR_t \leq PLR_{max} \quad (9)$$

$$q_{TES,t} = q_{TES,t}^{\wedge} - q_{TES,t}^{\vee} \quad (10)$$

$$Q_{TES,t} = \eta_{TES} Q_{TES,t-1} + q_{TES,t} \Delta t \quad (11)$$

$$0 \leq Q_{TES,t} \leq Q_{TES,rated} \quad (12)$$

2.3. Life-Cycle Assessment

Figure 2 presents the framework of life-cycle economic analysis, structured as a nested-loop process. The outer loop iterates through every storage portfolio (defined as Scheme = 1 to N_s), each representing a different combination of BESS and TES capacities. For each individual scheme, the inner loop simulates the system entire operational lifespan, progressing year by year (from Year = 1 to lifespan). The annual simulation involves three critical sequential steps. First, the degradation model is applied to update the performance

characteristics of the storage components (e.g., BESS capacity, TES efficiency) based on their operational age. Second, the operation optimization of typical days is executed, using these degraded specifications, along with the weather data and TOU tariffs, to determine the optimal daily dispatch strategy. Thirdly, the results from these typical days are used to calculate the annual economic performance for that specific year. This process is repeated until the system's end-of-life is reached, providing a life-cycle economic analysis for each portfolio.

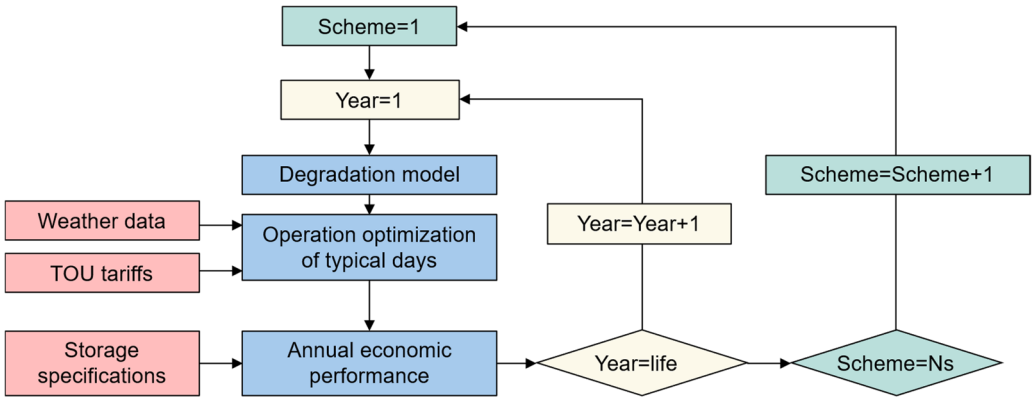


Figure 2. Framework of life-cycle economic analysis.

2.3.1. Degradation Models and Key Assessment Indicators

The life-cycle analysis incorporates degradation models for both electrical and cooling storage systems. As shown in Equation (13), the BESS is modeled with a linear reduction in its maximum capacity, assuming the battery reaches its end-of-life (defined as a 20% total capacity loss) over its specified lifespan. This simplified linear fade is applied annually and serves as a proxy for the combined effects of cycling and calendar-based aging. For the cooling storage, degradation is represented as a loss of storage efficiency over time. As shown in Equation (14), the efficiency in year i is reduced by a constant annual degradation factor from its initial value.

$$P_{EES,max,i} = P_{EES,max} * \left(1 - \frac{(i-1)}{L_{EES}} * 20\%\right) \tag{13}$$

$$\eta_{TES,i} = \eta_{TES} - (i-1) * \alpha \tag{14}$$

The economic viability of each alternative scheme is evaluated using two primary financial metrics: Life-Cycle Cost Saving (LCCS) and Discounted Payback Period (DPBP). The LCCS quantifies the total net present value of the investment over the project's financial timeline, by summing all discounted annual profits net of operation and maintenance costs, subtracting the initial investment and any future replacement costs, while adding the discounted residual value, as shown in Equation (15). A discount rate is applied to calculate future cash flows. The annual profit is the core driver of value, defined in Equation (17) as the total baseline annual energy cost (without storage systems) minus the optimized annual energy cost (with each scheme of storage systems). This optimized cost is derived from the results of the typical day clusters, weighted by the number of days in each cluster.

$$LCCS = \sum_{i=1}^{L} \frac{(Pro_i - C_{OM})}{(1+r)^i} - C_{INV} - C_{REP} + V_{RES} \tag{15}$$

$$C_{INV} = \sum_{i=1}^{DPB} \frac{(Pro_i - OM)}{(1+r)^i} \tag{16}$$

$$Pro_i = C_{base,i} - \sum_{d=1}^{k} (N_d * Cost_d) \tag{17}$$

2.3.2. Typical Day Selection

A primary challenge in system design is evaluating life-cycle performance, which requires operational optimization. Simulating the system operation across its entire multi-year lifespan is computationally infeasible. This complexity arises from the non-linear performance characteristics of components (e.g., chiller efficiency, battery degradation) which need to be calculated iteratively. To overcome this computational barrier, the K-means clustering method is adopted to select a small set of representative typical days to streamline the analysis [21]. As mentioned, numerous studies demonstrated the advantages of the K-means clustering method in typical day selection for energy system design. In this paper, the clustering method partitions 365 days into several clusters based on three daily features: the 24 h cooling load profile, the 24 h non-HVAC electricity load profile, and the 24 h PV generation profile. This process ensures that the selected typical days collectively capture the full range of seasonal and operational variations found in the annual dataset.

3. Validation Arrangement of Case Study

3.1. Test Scenario and Building Modeling

The proposed design method is validated based on the "hot summer and cold winter" climate zone, as this region presents a critical case for hybrid storage analysis. The hot summer results in substantial cooling demand that frequently aligns with high-price Time-of-Use (TOU) tariff periods and peak solar generation. Shanghai (31.2° N, 121.4° E) is selected as the representative city for this climate zone. To create a high-fidelity dataset, Rooftop PV generation is simulated via the System Advisor Model (SAM) [22], using Shanghai specific weather files (GHI, DHI, temperature) and a latitude-matched, south-facing panel orientation (31.2°). The PV system is specified as 1152 modules (36 parallel strings with 32 modules per string), each possessing a module power of 675 W (model CHSM66M-HC-675). This large array is connected to an inverter system rated at 837 kW (EPC Power Corp 50-100181). Figure 3 presents the monthly climatic characteristics of the case study location, including temporal trends of temperature and solar radiation.

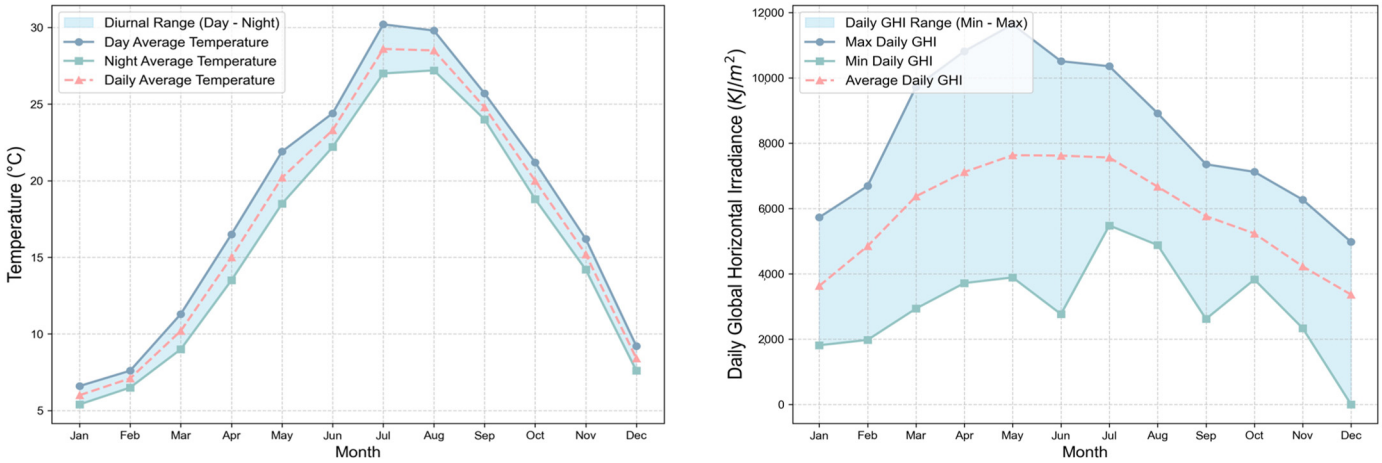


Figure 3. Monthly temperature profile and diurnal range (**left**); daily global horizontal irradiance (**right**) of Shanghai.

For this life-cycle analysis of optimal storage design, a representative medium-office building is selected as a standard prototype based on ASHRAE Standard 90.1 Prototype Building Models [23]. The corresponding building energy consumption (including cooling and electricity loads) is simulated using the TRNSYS18 platform [24]. This simulation integrates local climate data, detailed occupancy schedules, and the specific thermal properties of the envelope. The construction type features a wall thermal transmittance (U-value)

of 0.89 W/m^{2}K, a roof thermal transmittance of 0.54 W/m^{2}K, and a window thermal transmittance of 2.89 W/m^{2}K according to reference [25]. The window-to-wall ratio is set at 0.3. The internal loads are assumed as lighting load at 12 W/m^2, equipment load at 15 W/m^2, and occupancy load of 130 W/person (corresponding to a density of 10 m^2 per person). For indoor design conditions, the building maintains a constant temperature and humidity setpoint of 24 °C and 60% RH, respectively, during standard office hours from 8:00 to 18:00. The specifications for the electric chiller are sized at 1.2 times the peak cooling load of the building. Its dynamic operational characteristics are modeled, and the coefficients are empirically derived by fitting the quadratic function to performance curves provided by equipment manufacturers (e.g., Carrier 30XA 252–1702), being set as n_1 = 0.0523, n_2 = 0.9825, and n_3 = 0.0303.

3.2. Different TOU Tariff Scenarios and Specifications of Storage System

Figure 4 shows the reference of the Time-of-Use tariff in the current Shanghai electricity market. It is noted that grid agencies in the same region sometimes update electricity tariffs, which may affect storage investment strategies. Therefore, a set of scenarios is generated by varying the critical peak price and peak-to-valley (off-peak) ratio for comparative analysis, as shown in Table 1, and the shoulder rate of the reference tariff is held constant at 0.794 RMB/kW. Figure 5 shows TOU tariffs generated for 13 different scenarios in comparative optimization analysis. Table 2 lists the specifications and parameters of the storage system for the life cycle analysis. During the performance assessment, the initial investment of the project is RMB 3 million with a timeline of 20 years and discount rate of 4%.

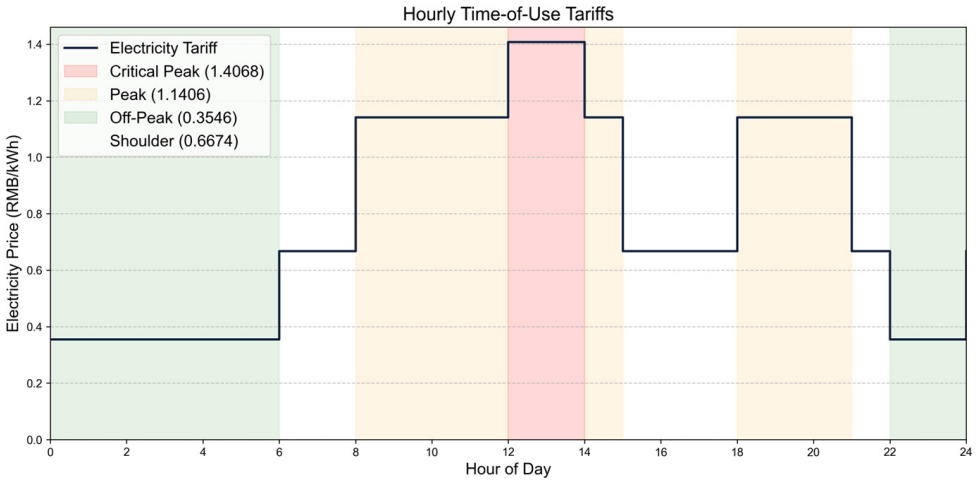


Figure 4. Time-of-Use tariff structures of Shanghai electricity market.

Table 1. Different scenarios of TOU tariffs for comparative analysis.

Scenario	Critical Peak	Peak	Shoulder	Off-Peak (Valley)	Peak-to-Valley Ratio
1	-	-	0.667	-	1.00
2	1.112	0.768	0.667	0.512	1.50
3	1.211	0.964	0.667	0.482	2.00
4	1.281	0.980	0.667	0.392	2.50
5	1.255	0.908	0.667	0.363	2.50
6	1.324	1.026	0.667	0.342	3.00
7	-	1.141	0.667	0.313	3.65

Table 1. *Cont.*

Scenario	Critical Peak	Peak	Shoulder	Off-Peak (Valley)	Peak-to-Valley Ratio
8	1.407	1.141	0.667	0.313	3.65
9	1.543	1.156	0.667	0.289	4.00
10	1.657	1.405	0.667	0.281	5.00
11	1.767	1.644	0.667	0.274	6.00
12	1.898	1.834	0.667	0.262	7.00
13	2.201	2.048	0.667	0.256	8.00

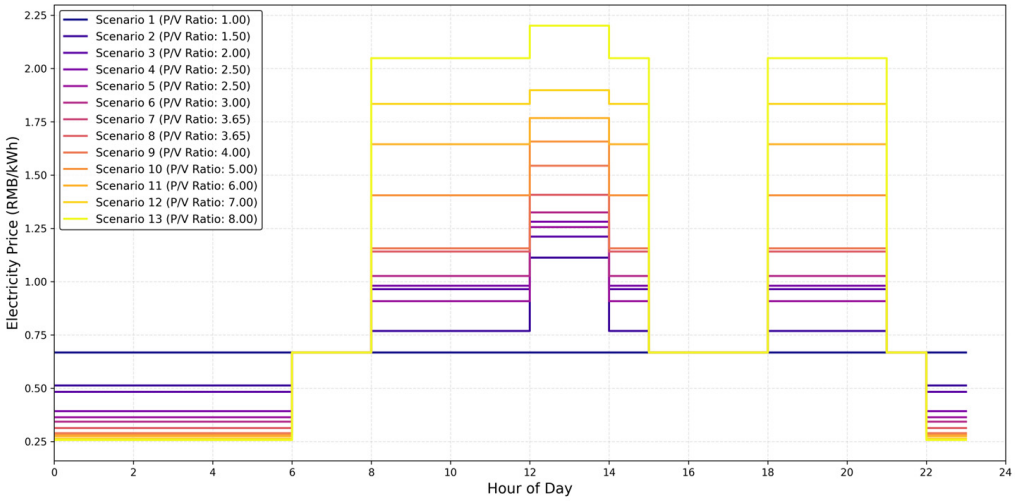


Figure 5. Time-of-Use tariffs for different scenarios of Shanghai electricity market.

Table 2. Specifications and parameters of storage systems [7].

System	Description	Value	Unit
TES	Capacity cost	70.3–281.3	RMB/kWhc
	Storage duration	8	h
	Operation and maintenance cost	0.7% of investment cost	per year
	Energy storage efficiency	0.998	-
	Lifespan	20	years
	Efficiency degradation rate α	0.002	-
BESS	Capacity cost	984.2~1687.2	RMB/kWhe
	Storage duration	2	h
	Operation and maintenance cost	0.5% of investment cost	per year
	Calendar life (normal corrosion)	10 [26]	years
	Charging/discharging efficiency	0.95	-

4. Results and Analysis

The operation of building energy systems without energy storage systems is considered as the baseline scenario. *K*-means clustering for typical day selection is conducted in Python 3.13. The life-cycle optimization of the building energy system is programmed via YALMIP in a MATLAB 2023 environment and solved by Gurobi solver using a computer with an eight-core Intel Core i7 CPU.

4.1. Clustering Results for Selecting Typical Days

The K-means clustering method is adopted to select typical days (TD) based on three daily features as mentioned in Section 2.3.2, and the clustering results are presented in Figure 6. It divides the annual operating conditions into 12 different profiles based on

the 24 h patterns of PV generation, cooling load, and other electricity loads. The number of days corresponding to each TD, such as TD 1 (Days: 36), which indicates that 36 days conform to the pattern of Typical Day 1, is crucial for weighted annual calculations. The PV generation profiles in the left panel, such as those for TD 1 (36 days), show a clear bell-shaped curve with high midday peaks approaching 600 kW, representing sunny, high-yield days. In contrast, low PV days like TD 4 (35 days) and TD 12 (10 days) peak well below 200 kW. The distribution effectively captures the variability from sunny days to cloudy or rainy days. The cooling load profiles in the middle panel demonstrate high seasonal dependency, with peak cooling days (TD 5) reaching up to 5000 kW during the afternoon, reflecting intense summer conditions. In contrast, the other load is characterized by sharp, high-magnitude plateaus (e.g., TD 11) indicating standard operation, whereas other clusters (e.g., TD 2, TD 6) show only a low, flat base load, representing non-operational or holiday periods. This set of 12 profiles effectively captures the necessary operating variability for the life-cycle optimization model. To validate the K-means clustering approach, the total annual baseline operational costs were calculated and compared for two scenarios: the whole-year operation and the representative typical days operation (where each typical day's cost was scaled by the number of similar days it represents). The comparison yielded a minimal difference of 0.03%, which is acceptable for reducing optimization scenarios without negligibly impacting overall results.

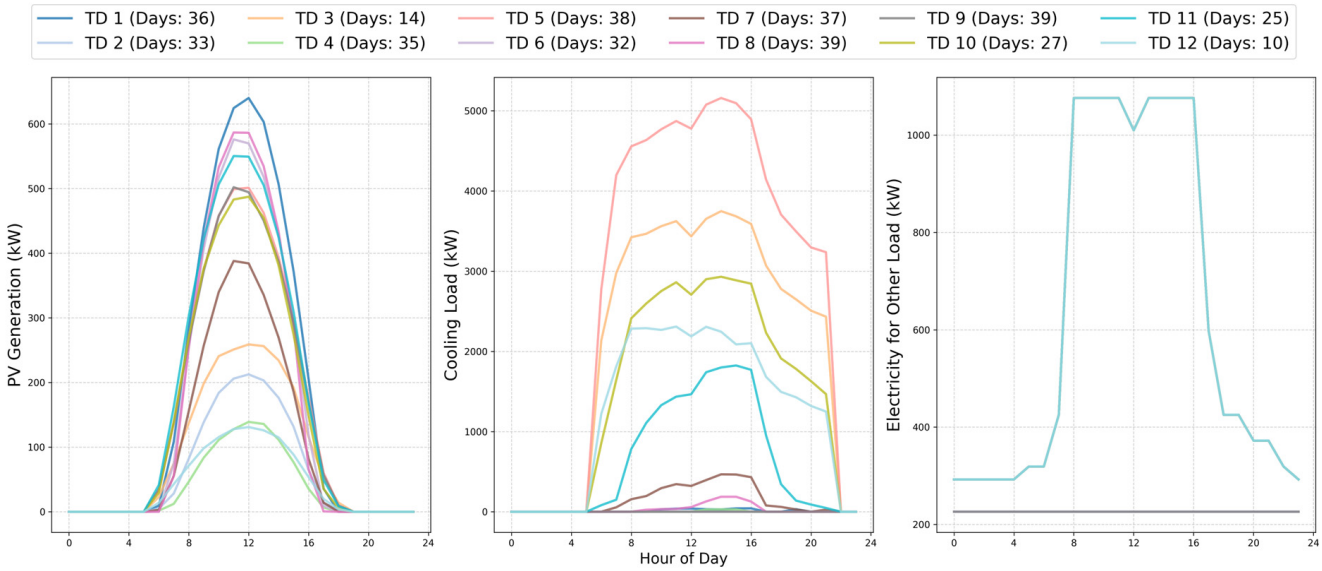


Figure 6. Typical daily load profiles based on *K*-means clustering.

4.2. Optimization Results of Hybrid Storage Systems

4.2.1. Operation Optimization of Typical Days

For each typical day, the operation of the storage system is optimized to maximize the economic benefits under corresponding TOU tariffs. The optimal operation results of hybrid storage systems for typical day 3 under scenario 8 are shown in Figures 7 and 8. The initial investment in storage systems is RMB 3 million with an allocation of 44.44% for cooling storage and 55.56% for electrical storage. It can be seen from Figure 7 that the grid-imported electricity is optimized by utilizing the storage systems according to the TOU and feed-in tariffs. The total electricity load is satisfied by a combination of on-site PV generation, grid import, and battery discharging. The battery is primarily charged during the off-peak hours when the electricity price is lowest. During the high-price critical-peak hours, the electricity imported from the power grid is significantly minimized. Figure 8 shows the hourly cooling balance of the building. In the presented typical day, relying

solely on discharging the cooling storage during the daytime is insufficient to fully meet the cooling load. Electric chillers are still operated throughout the day. TES is strategically charged during the off-peak periods, especially during the early hours (00:00–06:00). The stored cooling is then discharged during the high-demand daytime hours, particularly throughout peak and critical-peak hours.

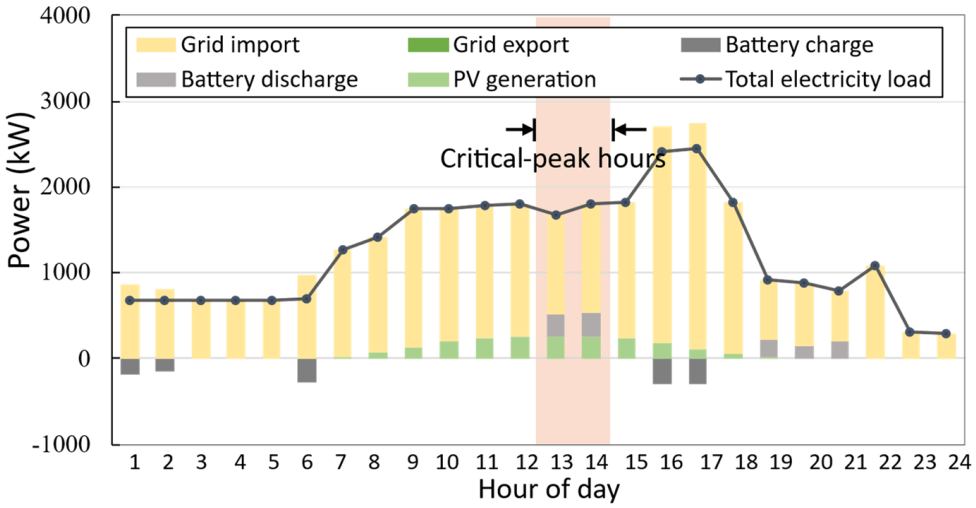


Figure 7. Electricity balance under operation optimization of typical day (TD = 3).

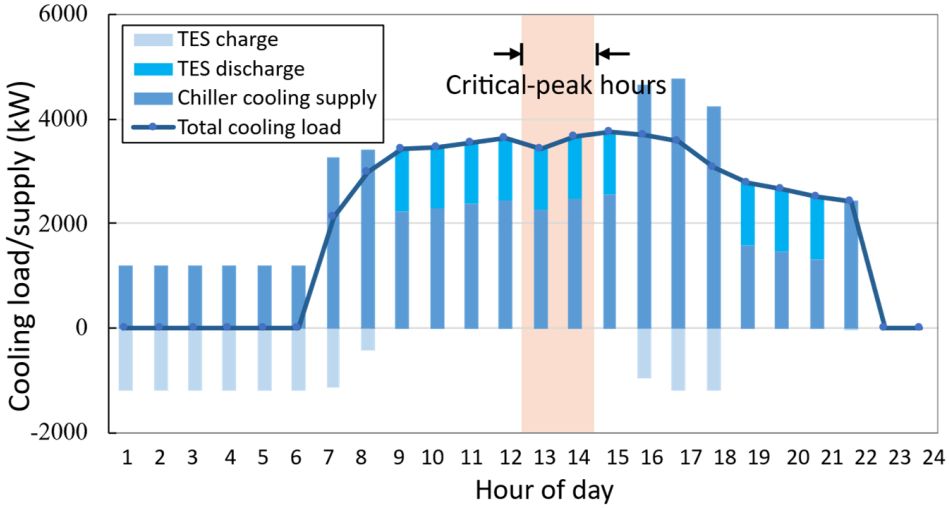


Figure 8. Cooling balance under operation optimization of typical day (TD = 3).

4.2.2. Optimal Hybrid Storage Portfolio Under Different TOU Tariffs

The life cycle economic analysis of hybrid storage systems considering the storage degradation is conducted by implementing iterative operation optimization over the project timeline. Figure 9 shows the results of the life cycle cost saving of hybrid storage systems under different TOU tariffs (S1–S13), with the optimal scheme highlighted with a gold border in each scenario. The schemes represent a compositional transition in the storage system, ranging from 100% cooling storage (Scheme 1) to 100% battery storage (Scheme 10). A clear shift can be found in the optimal portfolio as the P/V ratio increases. Under low P/V ratios (S1–S2), LCCS remains negative, which indicates the system incurs the minimum cost rather than generating savings. The storage system becomes economically beneficial when the P/V ratio rises above 2.00. While the P/V ratio is identical between S4 and S5, and between S7 and S8, S5 and S8 are characterized by a higher critical price, which provides a greater arbitrage opportunity, enabling these scenarios to achieve higher LCCS. As the P/V

ratio rises, the optimal scheme quickly transitions to battery-dominant configurations. For S9–S13 with high P/V ratios, Schemes 7 and 8 emerge as the most cost-effective portfolios, which peak at RMB 12,313,038 in S13. This transition shows that larger price differentials between peak and valley periods significantly enhance the profitability of battery storage systems due to the quick response capabilities for maximizing arbitrage revenues.

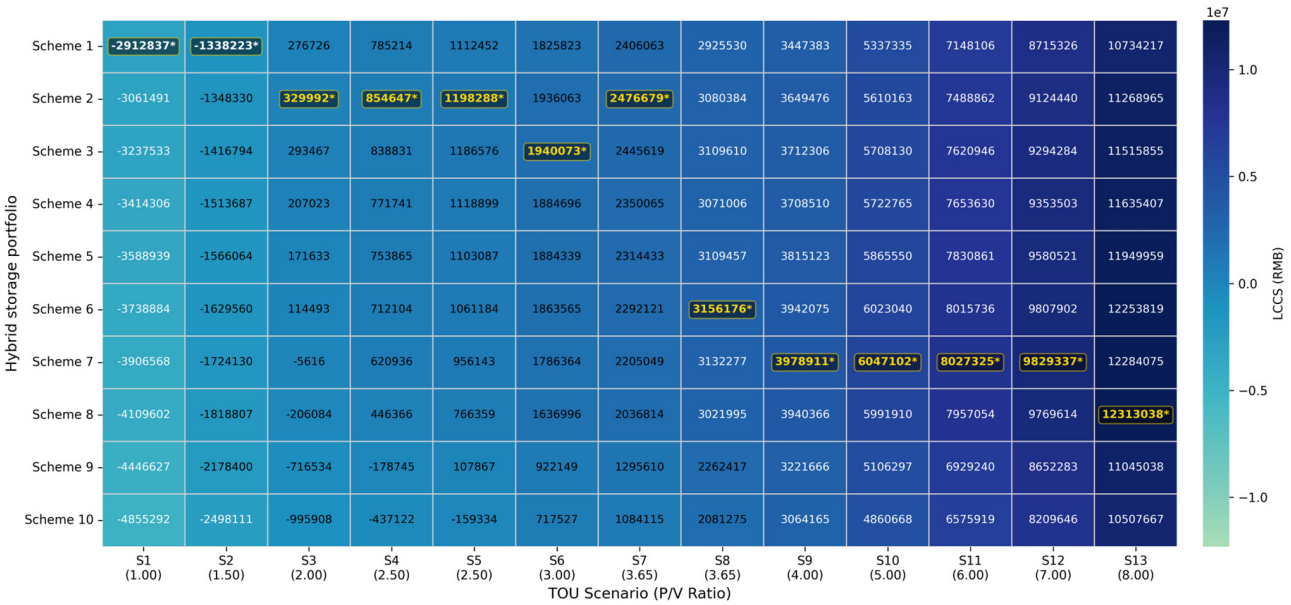


Figure 9. Life cycle cost saving of hybrid storage systems under different TOU tariffs (* represents the best portfolio under each scenario).

Table 3 summarizes the results for optimal investment allocations between cooling storage and electrical storage based on life cycle cost savings under various TOU tariff scenarios. The table also includes the corresponding discounted payback period for each optimal scheme. Economic savings begin at S3 (P/V = 2.00), where the optimal scheme is dominated by cooling storage at 88.89%, achieving an initial LCCS of RMB 329,991.93 and a DPBP of 16.53 years. An obvious difference is observed between the optimal schemes of S7 (88.89% cooling storage) and S8 (55.56% battery storage), despite both sharing the same P/V ratio of 3.65. This sharp transition indicates that the higher critical price in S8 serves as the decisive factor, pushing the optimal scheme towards cooling storage dominance. This is because the duration of the critical price period is limited and coincides with periods of high cooling demand, enabling the cooling storage system to minimize the electricity consumption of chillers.

Figure 10 presents the discounted payback periods (DPBP) for ten hybrid storage schemes under different TOU tariffs. The color gradient uses a sequential map where darker shades represent a shorter and financially better payback period. As the P/V ratio increases, the DPBP for all schemes shortens significantly, with the shortest payback periods consistently achieved by the battery-dominant schemes under S8–S13. While the LCCS analysis under S5–S7 indicates that cooling storage-dominant schemes offer the best long-term economic gains, the corresponding DPBP analysis shows better performance of the battery-dominant Scheme 7. This is because battery storage can generate higher arbitrage revenues at the early stage, but the advantage is eventually mitigated by the later costs associated with battery degradation and necessary replacement. The hybrid storage investment decision necessitates a multi-criteria evaluation considering both LCCS and DPBP as the optimal portfolio may differ upon the investor's specific strategic objectives.

Table 3. Results of optimal storage portfolio considering life cycle cost savings.

Scenario	P/V Ratio	Cooling Storage	Battery Storage	LCCS	DPBP
1	1.00	0.00%	0.00%	-	-
2	1.50	0.00%	0.00%	-	-
3	2.00	88.89%	11.11%	329,991.93	16.53
4	2.50	88.89%	11.11%	854,646.82	13.33
5	2.50	88.89%	11.11%	1,198,287.95	9.69
6	3.00	77.78%	22.22%	1,940,072.69	7.95
7	3.65	88.89%	11.11%	2,476,678.68	7.29
8	3.65	44.44%	55.56%	3,156,176.34	6.17
9	4.00	33.33%	66.67%	3,978,911.34	5.36
10	5.00	33.33%	66.67%	6,047,102.24	4.16
11	6.00	33.33%	66.67%	8,027,325.16	3.43
12	7.00	33.33%	66.67%	9,829,336.87	2.95
13	8.00	22.22%	77.78%	12,313,038.33	2.48

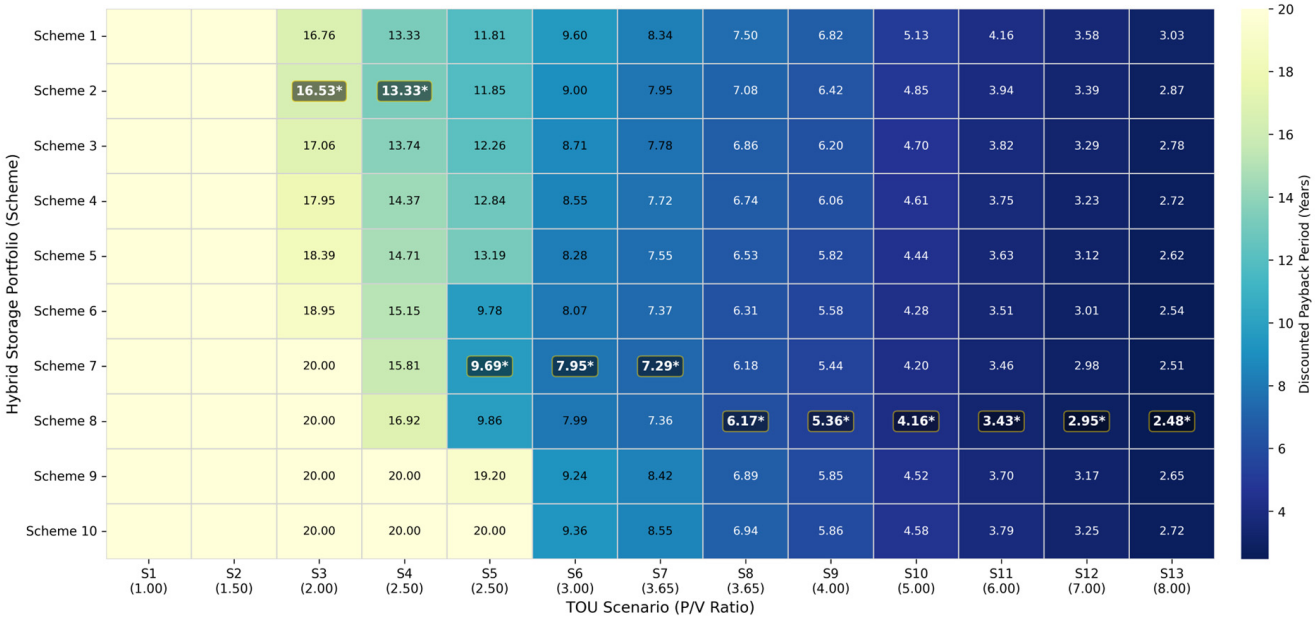


Figure 10. Discounted payback periods of hybrid storage systems under different TOU tariffs (* represents the best portfolio under each scenario).

4.2.3. Optimal Hybrid Storage Portfolio Under Different Storage Costs

To investigate the impact of storage capacity costs on the optimal hybrid storage portfolio, we conducted the life cycle economic analysis for each scheme under varying battery and cooling storage capacity costs. The TOU scenario adopted is based on the current real tariff in Shanghai, i.e., Scenario 8 (P/V ratio = 3.65). The results for different hybrid storage schemes, as presented in Figure 11, provide valuable insights into the economic performance of storage systems under varying market conditions. The impacts of two key variables are examined: (a) battery capacity costs and (b) cooling storage capacity costs, both of which play significant roles in determining the financial feasibility and optimal portfolio of energy storage systems.

Figure 11a presents the life cycle cost savings under different battery capacity costs, ranging from 140 USD/kWhe to 260 USD/kWhe. As the price of battery storage increases, the potential savings decrease across all storage schemes, which indicates the sensitivity of hybrid storage systems to fluctuations in battery costs. However, when the battery capacity cost is below 180 USD/kWhe, the optimal portfolio consistently remains as Scheme 8. For Scheme 10, which is 100% battery storage, life cycle cost savings increase as the

battery price decreases, yet hybrid storage still demonstrates the most favorable economic performance. When the battery capacity cost exceeds 200 USD/kWhe, hybrid schemes with a dominant cooling storage component begin to show better life cycle cost savings. At a battery capacity cost of 260 USD/kWhe, 100% cooling storage offers the best economic performance, indicating that battery storage has lost its economic feasibility.

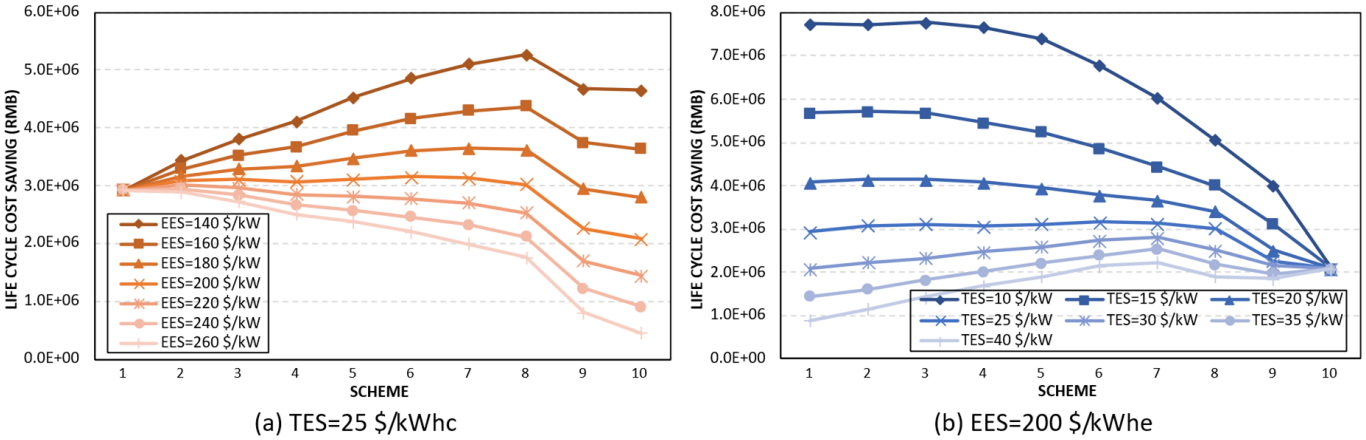


Figure 11. Life cycle cost saving of different hybrid storage schemes with various (**a**) battery capacity costs and (**b**) cooling storage capacity costs.

Figure 11b presents the life cycle cost savings under different cooling storage capacity costs, ranging from 10 USD/kWhc to 40 USD/kWhc. As the cost of cooling storage increases, the life cycle cost saving of all schemes generally decreases. The optimal portfolio is dominated by cooling storage, but even when the cooling storage capacity cost is below 15 USD/kWh, the optimal portfolio does not shift to purely cooling storage. This is because the benefits of cooling storage are constrained by the capacity of the chiller, making hybrid storage the better choice. When the cooling storage capacity cost exceeds 20 USD/kWhc, the optimal portfolio shifts towards a battery-dominant scheme.

5. Conclusions

This study systematically investigates the sensitivity of optimal hybrid storage system portfolios combining battery and cooling storage to varying Time-of-Use tariffs and storage capacity costs in office buildings in a 'hot summer and cold winter' climate zone. The proposed method can be easily adapted to other building types in different climate zones. The main conclusions of this study are summarized as follows:

- A multi-scenario, life-cycle optimization framework is developed by incorporating daily operation optimization model considering storage degradation and system dynamic efficiencies. A multi-criteria evaluation considering both life-cycle cost savings and the discounted payback period is effective and required for the investment decision. While battery-dominant schemes generally achieve the shortest DPBP (as low as 2.48 years in S13), cooling storage-dominant schemes can sometimes offer better long-term LCCS under medium P/V ratios (S5–S7) due to battery degradation and replacement costs.
- The economic viability of the storage system is highly sensitive to the structure of the TOU tariff, particularly the P/V ratio and the presence of critical-peak pricing. As the P/V ratio increases, the profitability of the storage system is significantly enhanced, driving the optimal portfolio towards battery-dominant schemes due to its quick response capabilities. When the P/V ratio is at intermediate levels, the presence of a

high critical price period, which is typically limited and coincides with high cooling demand, pushes the optimal portfolio towards cooling storage dominance.

- The optimal portfolio is highly sensitive to storage capacity cost fluctuations. An increase in battery capacity cost beyond 200 USD/kWhe can cause the optimal scheme to shift towards cooling storage-dominant portfolios. Conversely, if the cooling storage capacity cost exceeds 20 USD/kWhc, the optimal portfolio shifts back to battery-dominant schemes.

Author Contributions: Conceptualization, H.T.; methodology, H.T. and Y.Z.; software, H.T.; validation, H.T. and Y.Z.; formal analysis, H.T. and Y.Z.; investigation, H.T. and Z.Z.; writing—original draft preparation, H.T.; writing—review and editing, Z.Z.; funding acquisition, H.T. All authors have read and agreed to the published version of the manuscript.

Funding: This research presented in this paper is financially supported by a Start-up Fund P0056561 under the Strategic Hiring Scheme of The Hong Kong Polytechnic University.

Data Availability Statement: The data presented in this study is available on request from the authors due to the pravicy.

Conflicts of Interest: The authors declare no conflicts of interest.

Abbreviations

The following abbreviations and nomenclature are used in this manuscript:

PV	Photovoltaic
TOU	Time-of-Use tariff
FIT	Feed-in tariff
TES	Thermal energy storage
BESS	Battery energy storage systems
SOC	State of Charge of battery
COP	Coefficient of performance
HVAC	Heating, ventilation and air conditioning
LCCS	Life cycle cost saving
DPBP	Discounted payback period
PLR	Part load ratio
GHI	Global horizontal irradiance
DHI	Diffuse horizontal irradiance
TD	Typical day
$P_{grid,t}$	Power imported from the grid
$G_{grid,t}$	Power exported to the grid
$P^{\wedge}_{EES,t}$	Charging rate of battery
$P^{\vee}_{EES,t}$	Discharging rate of battery
η_{ch}	Charging efficiency
η_{dis}	Discharging efficiency
$q_{cooling,t}$	Cooling load
q_{rated}	Rated cooling capacity of chiller
$q^{\wedge}_{TES,t}$	Charging rate of thermal energy storage
$q^{\vee}_{TES,t}$	Discharging rate of thermal energy storage
$Q_{TES,t}$	Stored energy
η_{TES}	Storage efficiency
$Q_{TES,rated}$	Rated storage capacity

References

1. Impram, S.; Varbak Nese, S.; Oral, B. Challenges of renewable energy penetration on power system flexibility: A survey. *Energy Strategy Rev.* **2020**, *31*, 100539. [CrossRef]

2. Wang, Q.; Hodge, B.-M. Enhancing Power System Operational Flexibility with Flexible Ramping Products: A Review. *IEEE Trans. Ind. Inform.* **2017**, *13*, 1652–1664. [CrossRef]
3. Tang, H.; Wang, S.; Li, H. Flexibility categorization, sources, capabilities and technologies for energy-flexible and grid-responsive buildings: State-of-the-art and future perspective. *Energy* **2021**, *219*, 119598. [CrossRef]
4. IEA. *Energy Efficiency 2024*; International Energy Agency: Paris, France, 2024. Available online: https://www.iea.org/reports/energy-efficiency-2024 (accessed on 10 November 2025).
5. Costa, R.; Silva, R.; Faia, R.; Gomes, L.; Faria, P.; Vale, Z. Empowering energy management in smart buildings: A comprehensive study on distributed energy storage systems for Sustainable consumption. *Energy Build.* **2024**, *324*, 114953. [CrossRef]
6. Zhang, S.; Ocłoń, P.; Klemeš, J.J.; Michorczyk, P.; Pielichowska, K.; Pielichowski, K. Renewable energy systems for building heating, cooling and electricity production with thermal energy storage. *Renew. Sustain. Energy Rev.* **2022**, *165*, 112560. [CrossRef]
7. Tang, H.; Wang, S. Life-cycle economic analysis of thermal energy storage, new and second-life batteries in buildings for providing multiple flexibility services in electricity markets. *Energy* **2023**, *264*, 126270. [CrossRef]
8. Li, J. Optimal sizing of grid-connected photovoltaic battery systems for residential houses in Australia. *Renew. Energy* **2019**, *136*, 1245–1254. [CrossRef]
9. Zhang, Y.; Ma, T.; Elia Campana, P.; Yamaguchi, Y.; Dai, Y. A techno-economic sizing method for grid-connected household photovoltaic battery systems. *Appl. Energy* **2020**, *269*, 115106. [CrossRef]
10. Liu, X.; Gou, Z. Hybrid forecasting and optimization framework for residential photovoltaic-battery systems: Integrating data-driven prediction with multi-strategy scenario analysis. *Build. Simul.* **2025**, *18*, 1587–1609. [CrossRef]
11. Amini, M.; Khorsandi, A.; Vahidi, B.; Hosseinian, S.H.; Malakmahmoudi, A. Optimal sizing of battery energy storage in a microgrid considering capacity degradation and replacement year. *Electr. Power Syst. Res.* **2021**, *195*, 107170. [CrossRef]
12. Jiang, Y.; Kang, L.; Liu, Y. Optimal configuration of battery energy storage system with multiple types of batteries based on supply-demand characteristics. *Energy* **2020**, *206*, 118093. [CrossRef]
13. Zhao, W.; Peng, J.; Cao, J.; Yin, R.; Song, J.; Yuan, Y. Characterization and prediction of demand response potential of air conditioning systems integrated with chilled water storage. *Energy Build.* **2024**, *323*, 114805. [CrossRef]
14. Tarragona, J.; Pisello, A.L.; Fernández, C.; Cabeza, L.F.; Payá, J.; Marchante-Avellaneda, J.; de Gracia, A. Analysis of thermal energy storage tanks and PV panels combinations in different buildings controlled through model predictive control. *Energy* **2022**, *239*, 122201. [CrossRef]
15. Zang, X.; Li, H.; Wang, S. Optimal design of energy-flexible distributed energy systems and the impacts of energy storage specifications under evolving time-of-use tariff in cooling-dominated regions. *J. Energy Storage* **2023**, *72*, 108462. [CrossRef]
16. Chen, Q.; Kuang, Z.; Liu, X.; Zhang, T. Optimal sizing and techno-economic analysis of the hybrid PV-battery-cooling storage system for commercial buildings in China. *Appl. Energy* **2024**, *355*, 122231. [CrossRef]
17. Niu, J.; Tian, Z.; Lu, Y.; Zhao, H. Flexible dispatch of a building energy system using building thermal storage and battery energy storage. *Appl. Energy* **2019**, *243*, 274–287. [CrossRef]
18. Tian, Z.; Wang, Y.; Li, X.; Wen, L.; Niu, J.; Lu, Y. Typical daily scenario extraction method based on key features to promote building renewable energy system optimization efficiency. *Renew. Energy* **2024**, *236*, 121420. [CrossRef]
19. Hemmati, S.; Ghaderi, S.F.; Ghazizadeh, M.S. Sustainable energy hub design under uncertainty using Benders decomposition method. *Energy* **2018**, *143*, 1029–1047. [CrossRef]
20. Schütz, T.; Schraven, M.H.; Fuchs, M.; Remmen, P.; Müller, D. Comparison of clustering algorithms for the selection of typical demand days for energy system synthesis. *Renew. Energy* **2018**, *129*, 570–582. [CrossRef]
21. Elsido, C.; Bischi, A.; Silva, P.; Martelli, E. Two-stage MINLP algorithm for the optimal synthesis and design of networks of CHP units. *Energy* **2017**, *121*, 403–426. [CrossRef]
22. Blair, N.; DiOrio, N.; Freeman, J.; Gilman, P.; Janzou, S.; Neises, T.; Wagner, M. *System Advisor Model (SAM) General Description (Version 2017.9.5)*; National Renewable Energy Laboratory (NREL): Golden, CO, USA, 2018. [CrossRef]
23. Goel, S.; Rosenberg, M.; Athalye, R.; Xie, Y.; Wang, W.; Hart, R.; Zhang, J.; Mendon, V. *Enhancements to ASHRAE Standard 90.1 Prototype Building Models*; Pacific Northwest National Laboratory (PNNL): Richland, WA, USA, 2014. [CrossRef]
24. Meiers, J.; Frey, G. Interfacing TRNSYS with MATLAB for Building Energy System Optimization. *Energies* **2025**, *18*, 255. [CrossRef]
25. Zhuang, C.; Wang, S. An adaptive full-range decoupled ventilation strategy for buildings with spaces requiring strict humidity control and its applications in different climatic conditions. *Sustain. Cities Soc.* **2020**, *52*, 101838. [CrossRef]
26. Lam, V.N.; Cui, X.; Stroebl, F.; Uppaluri, M.; Onori, S.; Chueh, W.C. A decade of insights: Delving into calendar aging trends and implications. *Joule* **2025**, *9*, 101796. [CrossRef]

Disclaimer/Publisher's Note: The statements, opinions and data contained in all publications are solely those of the individual author(s) and contributor(s) and not of MDPI and/or the editor(s). MDPI and/or the editor(s) disclaim responsibility for any injury to people or property resulting from any ideas, methods, instructions or products referred to in the content.